2013

# Enhanced microwave dielectric tunability of Ba0.5Sr0.5TiO3 thin films grown with reduced strain on DyScO3 substrates by three-step technique

Hongrui Liu
*Virginia Commonwealth University*

Vitaliy Avrutin
*Virginia Commonwealth University*, vavrutin@vcu.edu

Congyong Zhu
*Virginia Commonwealth University*

***See next page for additional authors***



Liu, H., Avrutin, V., & Zhu, C., et al. Enhanced microwave dielectric tunability of Ba0.5Sr0.5TiO3 thin films grown with reduced strain on DyScO3 substrates by three-step technique. Journal of Applied Physics, 113, 044108 (2013).

# Enhanced microwave dielectric tunability of $Ba_{0.5}Sr_{0.5}TiO_3$ thin films grown with reduced strain on $DyScO_3$ substrates by three-step technique

Hongrui Liu,[1] Vitaliy Avrutin,[1] Congyong Zhu,[1] Ümit Özgür,[1] Juan Yang,[2] Changzhi Lu,[2] and Hadis Morkoç[1]
[1]*Department of Electrical and Computer Engineering, Virginia Commonwealth University, Richmond, Virginia 23284, USA*
[2]*College of Electronic Information and Control Engineering, Beijing University of Technology, Beijing 100124, China*

(Received 8 October 2012; accepted 7 January 2013; published online 25 January 2013)

Tunable dielectric properties of epitaxial ferroelectric $Ba_{0.5}Sr_{0.5}TiO_3$ (BST) thin films deposited on nearly lattice-matched $DyScO_3$ substrates by radio frequency magnetron sputtering have been investigated at microwave frequencies and correlated with residual compressive strain. To reduce the residual strain of the BST films caused by substrate clamping and improve their microwave properties, a three-step deposition method was devised and employed. A high-temperature deposition at 1068 K of the nucleation layer was followed by a relatively low-temperature deposition (varied in the range of 673–873 K) of the BST interlayer and a high-temperature deposition at 1068 K of the top layer. Upon post-growth thermal treatment at 1298 K the films grown by the three-step method with the optimized interlayer deposition temperature of 873 K exhibited lower compressive strain compared to the control layer (−0.002 vs. −0.006). At 10 GHz, a high dielectric tunability of 47.9% at an applied electric field of 60 kV/cm was achieved for the optimized films. A large differential phase shift of 145°/cm and a figure of merit of 23°/dB were obtained using a simple coplanar waveguide phase shifter at 10 GHz. The low residual strain and improved dielectric properties of the films fabricated using the three-step deposition technique were attributed to reduced clamping of the BST films by the nearly lattice-matched substrate. © *2013 American Institute of Physics*. [http://dx.doi.org/10.1063/1.4789008]

## INTRODUCTION

Tunable phase shifters are of great interest for a wide variety of military and commercial applications, including communication satellites, phased array radars, and wireless local area networks.[1,2] Because the performance of the traditional phase shifters is limited due to the slow response of ferrites on the one hand and high insertion loss of the PIN diode on the other, ferroelectric thin film phase shifters have attracted a great deal of attention owing to inherent advantages, such as low cost, low power consumption, fast response time, and device miniaturization.[3] Ferroelectric $Ba_xSr_{1-x}TiO_3$ has been considered as one of the promising materials owing to its strongly electric-field-dependent permittivity.[4,5] Among all its compositions $Ba_{0.5}Sr_{0.5}TiO_3$ (BST) with Curie temperature of about 250 K has attracted a particular interest due to its paraelectric nature at room temperature as well as its high dielectric tunability and relatively low loss at microwave frequencies.[6]

In order for them to improve the performance of phase shifters, ferroelectric thin films need to possess high dielectric tunability and low loss, which is significantly affected by film strain.[7] To achieve films with high structural quality and low residual strain, both the selection of optimum substrates and optimizing the film deposition process are critical. To enhance structural quality, substrates of choice must have small lattice mismatch and similar thermal expansion to BST as well as both low dielectric constant and low dielectric loss which are required for microwave applications. BST thin films have, heretofore, mostly been deposited on substrates such as sapphire, MgO, $LaAlO_3$, and $SrTiO_3$,[8–10] $DyScO_3$ (DSO) is one of the best suitable candidates owing to its pseudocubic in-plane lattice parameter of 3.945 Å on (101) plane, which is very close to 3.947 Å of bulk BST, similar thermal expansion constant to BST ($\alpha_{DyScO3} = 8.4 \times 10^{-6}$ $K^{-1}$ and $\alpha_{BST} = 10.5 \times 10^{-6}$ $K^{-1}$), lack of phase transitions from 25 to 1273 K, and relatively low dielectric constant of ~20. However, when using substrates, which are nearly lattice-matched, as in the case of $DyScO_3$ or $SrTiO_3$, the in-plane lattice parameters of the epitaxial BST films are "clamped" to the lattice parameters of the substrate. Clamping would introduce a biaxial strain in the film, which plays an adverse role in the value of the dielectric constant as well as the achievable tunability. This twofold effect has been elaborated on previously.[11] Compressively strained BST films suffer from having not only an increased Curie temperature but also a lower dielectric constant tunability,[11,12] while the films under small tensile strain have improved relative permittivity and tuning.[11] In order to enhance the dielectric properties of BST thin films, much effort has been expended on optimizing the crystal structure by improving deposition techniques and growth conditions, such as tailoring the $Ar:O_2$ ratio of the growth atmosphere[13] or adding various buffer layers.[14,15]

A similar problem has been tackled in the field of SiGe growth on Si substrates, where highly relaxed films with low threading dislocation density are required for device applications. Among many approaches proposed to achieve virtually

 

compliant substrate,[16] the utilization of low-temperature buffer layer saturated with point defects of vacancy type was demonstrated to promote substantially strain relaxation while keeping dislocation density at relatively low level.[17]

In this work, we implemented the three-step deposition method on nearly lattice-matched $DyScO_3$ substrates, in which a compliant interlayer grown at relatively low substrate temperature is sandwiched between a thin nucleation layer and a relatively thick top layer both grown at higher temperature, in order to achieve BST films with low residual strain and high dielectric tunability at microwave frequencies. The improvement of the dielectric properties of the three-step grown BST thin films was correlated with the reduced residual strain assessed from high-resolution X-ray diffraction (HRXRD).

## EXPERIMENTAL DETAILS

BST thin films were deposited on $DyScO_3$ substrate by off-axis radio frequency (RF) magnetron sputtering. The deposition was carried out at a 120 W RF power and a pressure of 2 mTorr in a 6:1 $Ar/O_2$ gas mixture. To control the strain in BST films, a three-step growth technique was employed. First, a 70-nm-thick BST nucleation layer was deposited on the $DyScO_3$ substrate used at a relatively high temperature of $T_1 = 1068$ K. The substrate temperature was then decreased to $T_2$ within 30 min and a low-temperature BST interlayer of 180 nm in thickness was deposited. During the third and last step, the substrate temperature was increased back up to 1068 K ($T_3 = T_1$) within 30 min and a 450-nm-thick BST film was deposited as the topmost layer. The deposition temperature $T_2$ of the intermediate layer was varied and the structures with $T_2 = 873$, 773, and 673 K were grown (denoted as samples A, B, and C, respectively). A control sample (sample D) with a thickness of 700 nm was grown in a one step process at $T_1 = 1068$ K. To improve crystal quality further, all films were then annealed at 1298 K for 8 h in a tube furnace. An $O_2$ atmosphere ($O_2$ mass-flow rate of 20 sccm) was employed to prevent oxygen loss from BST films during the thermal anneal. This procedure was shown to alleviate strain and consequently enhance the dielectric properties.[13]

The crystal structure and orientation of the as-grown and annealed BST thin films were examined through the $2\theta$-$\omega$ scans by HRXRD using Cu K$\alpha$ radiation. The $2\theta$-$\omega$ scan was operated in the $2\theta$ scan range of 42°–69° with a step size of 0.002° and 5 s counting time per data point at 45 kV and 40 mA. The single-crystal BST (002) reflection and (022) reflection were observed in the symmetric and skew-symmetric $2\theta$-$\omega$ scan, respectively, on the as-grown and annealed epitaxial BST thin films. The reflections of the substrate were used as a calibration in the lattice-parameter calculation.

For the evaluation of dielectric properties, coplanar waveguides (CPWs) and interdigital capacitors (IDCs) with an electrode separation of 5 $\mu$m were photolithographically fabricated using a four-layer Cr/Ti/Ag/Au (50/25/2000/50 nm) metal stack. For the fabrication of the thick-metal electrodes, a tri-layer liftoff procedure using a PMMA/chromium/photoresist stack was employed to attain the CPW and IDC electrodes with the aid of electron-beam evaporation. More details of the fabrication procedure can be found in Ref. 18. The capacitance tuning of IDC devices was determined from capacitance-voltage (C-V) measurements performed in the voltage range of 0–40 V at a frequency of 1 MHz using a Hewlett-Packard 4284 LCR meter. Microwave measurements were conducted on the CPW devices with variable length transmission lines (0.2 mm to 1.4 mm). The width of the signal line was 60 $\mu$m and the gap between the signal line and the ground plate was 5 $\mu$m. The propagation parameters were measured using an HP 8510 C vector network analyzer in the frequency range from 2 to 20 GHz. A DC bias of up to 30 V was applied between the signal line and the ground plate to change the dielectric constant and induce the phase shift. The bias voltage of 30 V corresponds to a maximum applied electric field of 60 kV/cm for the 5 -$\mu$m-width gap between the signal line and the ground plane in CPW. The thru-reflect-line (TRL) calibration method[18] was employed to assess the dielectric constant, tunability, and phase shift of the BST films.

## RESULTS AND DISCUSSION

The out-of-plane and in-plane epitaxial relationships deduced from HRXRD measurements are (001) BST//(101) $DyScO_3$ and (100) BST//(010) $DyScO_3$, respectively, in agreement with findings by Diegalski *et al.*[19] for the growth of $SrTiO_3$ on $DyScO_3$. Figure 1 shows the XRD $2\theta$-$\omega$ scan of the symmetric (002) reflection from the as-grown samples (Figure 1(a)) and the annealed samples (Figure 1(b)). Unlike the control layer featuring only a single (002) reflection, the as-grown three-step film shows two peaks (Figure 1(a)), suggesting that the BST layers grown at different temperatures have different lattice parameters. Generally, the thicker the layer is the higher the reflection intensity is in HRXRD scan when the layers have comparable structural quality. We presume that the relatively more intense peak at $2\theta \approx 43.95°$ of as-grown film A is from the top 450-nm BST layer grown at $T_1 = 1068$ K, while the broader and weaker reflection is from the 180-nm-thick BST interlayer grown at $T_2 = 873$ K. The HRXRD pattern from the as-grown control film grown at the same temperature of 1068 K as that of the top layer in the three-step film A exhibits a single peak centered at 43.9°, close to that from the more intense peak for sample A in Figure 1(a). The seed layer most likely cannot be resolved on HRXRD scans due to its thinness (70 nm)/quality. Upon the thermal treatment at 1273 K for 8 h in flowing oxygen, two peaks observed for the as-grown film A merge into a single, asymmetric peak showing a small-angle tail (Figure 1(b)). The asymmetric shape of the reflection suggests the presence of a lattice-parameter gradient along the growth direction in the sample grown by the three-step method. Figure 1(b) shows the difference of the peak position from the BST (002) reflections of the annealed samples. Upon annealing the BST peaks shifted toward the DSO peaks, implying a lattice parameter reduction. The peak position of Film A is closer to DSO peak than the one of control Film D, corresponding to a smaller out-of-plane lattice parameter in Film A than in Film D.

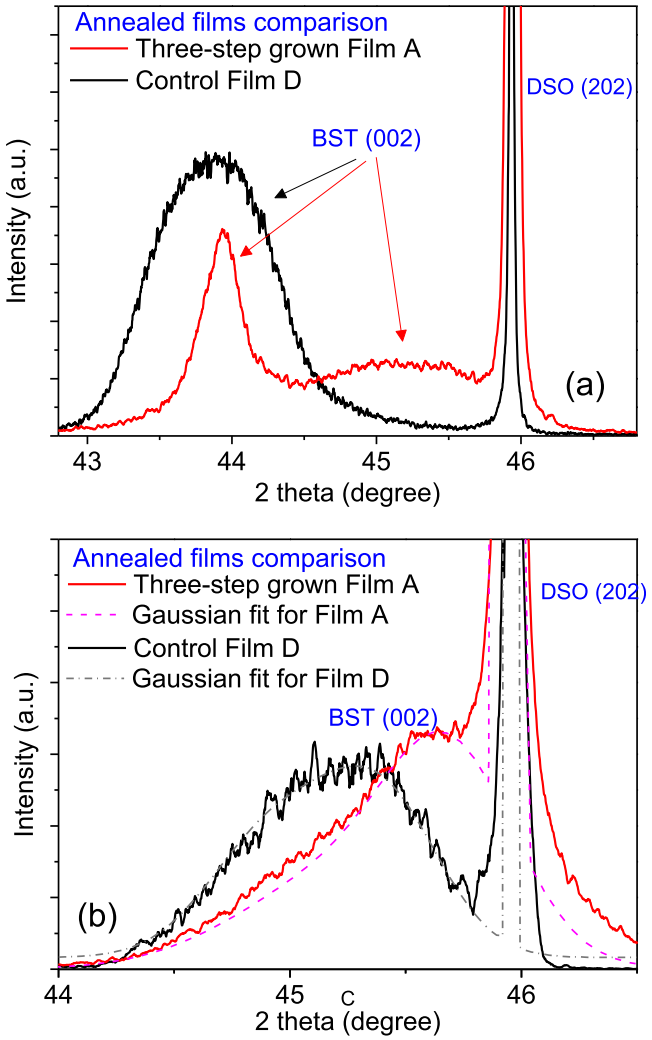


FIG. 1. HRXRD $2\theta$-$\omega$ scan of (002) reflection from (a) as-grown samples and (b) annealed samples. Red curves represent the three-step grown Film A and black curves represent the control Film D. The dashed lines represent the Gaussian fit for the films.

The out-of-plane, $c$, and in-plane, $a$, lattice parameters of the BST films were deduced from the symmetric (002) and skew-symmetric (022) reflections. To improve the accuracy in determination of the lattice parameters, diffraction (202) and (242) reflections from the $DyScO_3$ substrate were used as an internal standard in case of symmetric and skew-symmetric scans, respectively. The peak position and its experimental error were determined using Gaussian fit as shown in Figure 1(b). The lattice parameters of the annealed films so deduced are listed in Table I. Note that the lattice parameters of the films grown by the three-step method represent the top-most layer of the structure in accord with the abovementioned simulations of the asymmetric reflection curves. All the films showed a larger out-of-plane lattice parameter than their in-plane ones ($c > a$), indicative of compressive in-plane deformation. The presence of oxygen vacancies in the film and the lattice mismatch between the deposited layer and the substrate make the equilibrium (strain-free) lattice parameter of BST thin film different from the ideal bulk one. Thus, the ideal bulk lattice parameter (3.947 Å) should not be used in the film strain calculation.[20]

TABLE I. The lattice parameters and film strain of the three-step grown films (samples A, B, and C) and the control sample D upon post-deposition thermal treatment at 1298 K in $O_2$.

| Sample | $T_2$ (K) | $c$ (Å) | $a$ (Å) | Film strain $x_{1,2}$ |
|---|---|---|---|---|
| A | 873 | $3.989 \pm 0.008$ | $3.971 \pm 0.016$ | $-0.002 \pm 0.001$ |
| B | 773 | $3.987 \pm 0.009$ | $3.972 \pm 0.015$ | $-0.002 \pm 0.001$ |
| C | 673 | $4.007 \pm 0.011$ | $3.970 \pm 0.017$ | $-0.005 \pm 0.001$ |
| D | N/A | $4.004 \pm 0.011$ | $3.955 \pm 0.016$ | $-0.006 \pm 0.001$ |

In order to quantitatively describe film strain, we used an equilibrium (strain-free) lattice parameter $a_0$[21] instead of the BST bulk lattice parameter. The equilibrium lattice parameter $a_0$ is a function of the measured in-plane lattice parameter, $a$, and out-of-plane lattice parameter, $c$,: $a_0 = \left[c + 2\left(\frac{c_{12}}{c_{11}}\right)a\right] \Big/ \left[1 + 2\left(\frac{c_{12}}{c_{11}}\right)\right]$, where $c_{ij}$ are the elastic constants of BST, $c_{11} = 3.11645 \times 10^{11}\,\mathrm{N/m^2}$ and $c_{12} = 1.39805 \times 10^{11}\,\mathrm{N/m^2}$,[20] which are obtained by averaging the elastic constants of bulk $SrTiO_3$ and $BaTiO_3$ single crystals. The in-plane residual strain in the film is then given by $x_{1,2} = (a - a_0)/a_0$. All the films were found to exhibit compressive in-plane lattice distortion (film strain $x_{1,2} < 0$). Samples A and B have larger in-plane and smaller out-of-plane lattice parameters due to relatively small distortion ($x_{1,2} = -0.002$) as compared to the control one ($x_{1,2} = -0.006$ for sample D). This is attributed to generation of high concentration of point defects during the low temperature growth of the BST interlayer in the three-step deposition process, which facilitate the formation and propagation of dislocations, thus promoting strain relaxation.[17] With larger lattice parameters than the substrate, the interlayer partially compensates for the compressive strain in the top BST layer and reduces the mismatch between the top layer and the substrate. This mechanism is similar to the compliance effect: a thin freestanding substrate that shares the mismatch strain during the heteroepitaxy.[22] Upon post-deposition annealing, the point defects in the interlayer, especially the oxygen vacancies, were gradually reduced. The contracted lattice structure of the interlayer helps to relax the BST top layer. However, for the relatively low growth temperature of the interlayer (such as Film C), point defects generated in abundance may facilitate formation of stacking faults during the deposition, thus hardening the material.[17] Therefore, the choice of temperature used for the interlayer growth is important for high quality BST film deposition. However, further studies are warranted before the theoretical elucidation can be found for the interlayer effect on the BST film deposition.

The strain conditions of the BST films were correlated with the capacitance tuning of IDCs, $[C_{max}\text{-}C_{min}]/C_{max}$, determined from C-V measurements performed at 1 MHz in the $\pm 80$ kV/cm electric field range. As seen from Figure 2, the improvement in capacitance tuning of the film fabricated via the three-step method is consistent with the reduction of the film strain. The best tunability of 48%–49% was achieved for the films A and B, fabricated with $T_2 = 773$ K and 873 K, respectively, compared to 22% for the control

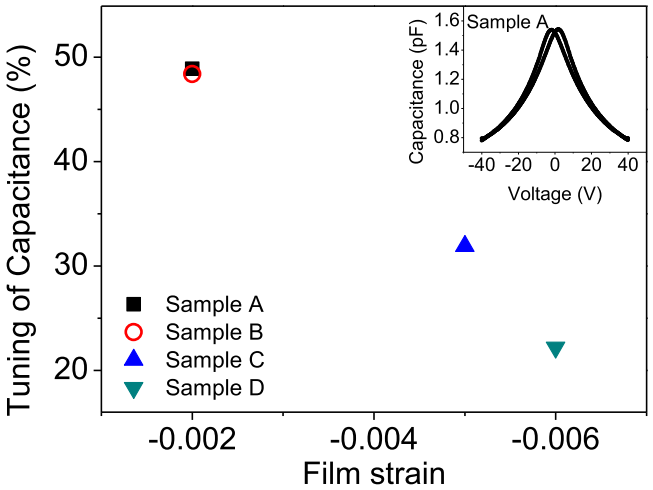


FIG. 2. The dependence of the tuning of the capacitance in 0-40 V at 1 MHz on the film strain. The inset shows the capacitance tuning for sample A.

layer. This implies that the three-step deposition with a proper interlayer growth temperature alleviates film strain and enhances tunability to a great extent.

In order to investigate the effect residual strain on the dielectric properties of the BST films on $DyScO_3$ substrates, the dielectric constant and tuning as well as the loss tangent of the film with the lowest strain (Film B fabricated by the three-step method with $T_2 = 773$ K) and the controlled sample (film D) were measured using CPW together with the conformal mapping technique.[23] As shown in Figure 3, the film employing the three-step-process, sample B, displayed relative dielectric constants as high as 1198, 1099, 1048, and large dielectric-constant tuning, defined by $[\varepsilon_r(0) - \varepsilon_r(V)]/\varepsilon_r(0)$ at an electric field of $E = 60$ kV/cm, of 50.7%, 47.9%, 45.8% at 5, 10, and 15 GHz, respectively. The control sample, Film D, exhibited maximum dielectric constants of only 1035, 956, 910, and dielectric-constant tuning values of 21.3%, 20.2%, 19.2% at 5, 10, and 15 GHz, respectively.

When the film suffers from a large compressive strain, the space for the in-plane ionic polarization associated with the displacement of $Ti^{4+}$ ion is limited by in-plane compression, resulting in relatively small dielectric constants.[24] The larger dielectric constant and the higher tunability exhibited by Film B is consistent with the reduced compressive strain compared with that in the control sample D. The dielectric constant value and tunability achieved for Film B is comparable to or even higher than those of BST thin films with comparable thickness deposited on other substrates, such as MgO or $LaAlO_3$ (LAO).[25,26]

Assuming that all of the loss in the system is ascribable to either conductor loss or dielectric loss, i.e., there is no radiation or surface wave losses, the tan $\delta$ of the BST layers can also be extracted. The dielectric loss tangent decreases with the electric field applied on the device and remained low (tan $\delta = 0.021$–$0.024$ at zero bias) for all films deposited by the three-step method. It should be noted that the top-most portion of the film has the major contribution to its microwave properties as well. Therefore, substantial improvement of the tunable dielectric properties of the BST films fabricated via the three-step technique compared to the control layer is consistent with the reduced compressive strain in the top most layer as revealed by HRXRD.

Another important characteristic of the ferroelectric film in microwave applications is the extent of the phase shift. Coplanar phase shifters formed on the three-step deposited films and the control film were studied at microwave frequencies. The differential phase shift per unit length measured on Film B at various electric fields is shown in Figure 4. At an electric field of 60 kV/cm, the differential phase shifts were 145.7°/cm and 256.1°/cm at 10 and 20 GHz, respectively, which were substantially higher than the corresponding values of 77.5°/cm and 142.7°/cm obtained on the control Film D. With the consideration of loss, the performance of phase shifters can be described using the figure of merit given by

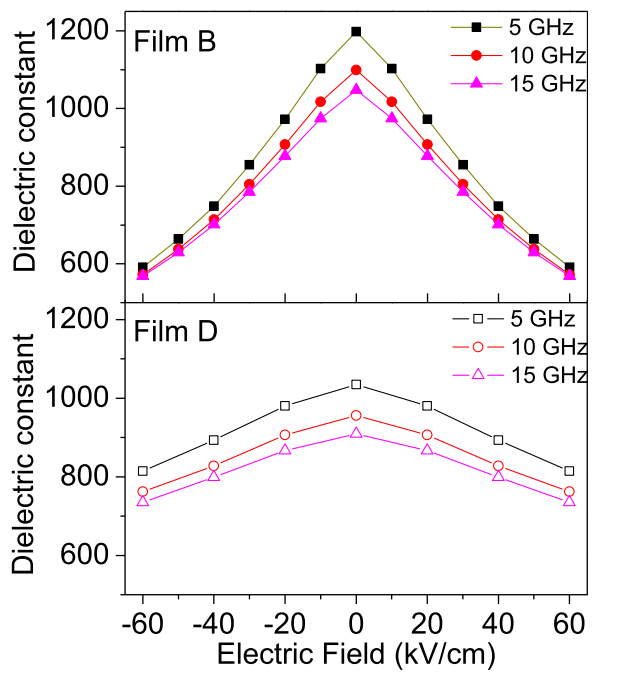


FIG. 3. Dielectric constant and its tuning of films B and D in the range of the electric field of 60 kV/cm at 5, 10, and 15 GHz, respectively.

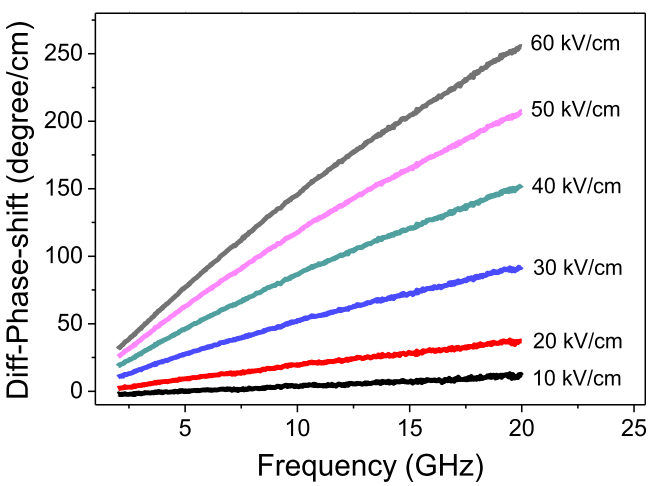


FIG. 4. The differential phase shift per unit length on CPW transmission line fabricated on sample B.

TABLE II. The film strain and microwave properties of the three-step deposited films (samples A, B, and C) and the control film (sample D). The differential phase shift and figure of merit were measured at an applied electric field of 60 kV/cm at 10 GHz.

| Sample | Film strain | Differential phase shift (°/cm) | Insertion loss (dB/cm) | Figure of merit (°/dB) |
|---|---|---|---|---|
| A | −0.002 | 145.2 | 6.3 | 23.0 |
| B | −0.002 | 145.7 | 6.7 | 21.7 |
| C | −0.005 | 132.6 | 16.5 | 8.0 |
| D | −0.006 | 77.5 | 10.0 | 7.7 |

$$\text{Figure of merit} = \frac{\varphi(V) - \varphi(0)}{IL}$$

where $\varphi(V)$ and $\varphi(0)$ are the differential phase shift under DC bias field of E and 0 V/cm, respectively, and IL represents the insertion loss per unit length. In the conformal mapping method, the insertion loss, derived from the scattering parameter $S_{21}$, is attributed to both the conductor loss from the transmission line and the dielectric loss from the film. Films A and B have relative low insertion loss of 6.3 and 6.7 dB/cm, respectively, while the control film showed a relative high insertion loss of 10.1 dB/cm. As shown in Table II, the structures deposited via the three-step method (Films A, B, and C) showed improvement in both the differential phase shift and the figure of merit compared with the control film D. The best performance was achieved on Films A and B deposited with $T_2 = 873$ K and 773 K, respectively, which showed a two-fold improvement over the control structure in terms of the differential phase shift (145°/cm vs. 77.5°/cm) and a three times enhancement of the figure of merit (23.0°/dB vs. 7.7°/dB). This differential phase shift is higher than the value of 90°/cm achieved on the much thicker, annealed (3-$\mu$m-thick) BST films using the same simple CPW geometry and applied field, while the figure of merit is only somewhat lower than that obtained in the latter case (23.0°/dB *vs.* 35°/dB).[18]

The improvement of BST-film-based phase shifter at microwave frequencies is consistent with the reduced film strain in the films fabricated by the three-step deposition technique. Although the mechanism responsible for the reduced film clamping by a nearly lattice-matched substrate requires further microscopic investigations, the experimental results obtained so far indicate the effectiveness of the implemented deposition method in achieving BST thin films with high microwave tunability.

## CONCLUSIONS

We investigated the dielectric properties of BST films on nearly lattice-matched $DyScO_3$ substrates deposited using a three-step method. High values of both dielectric constant (1099) and its electric-field tuning (47.9% at 10 GHz and $E_{DC} = 60$ kV/cm) were achieved for the annealed films fabricated with the optimized interlayer deposition temperature of 873 K. Coplanar phase shifters based on the three-step deposited films exhibited a two-fold enhancement in differential phase shift (145°/cm *vs.* 77.5°/cm) and a three time higher microwave figure of merit (23°/dB vs. 7.7°/dB) compared with the control sample deposited in a single step at 1068 K. The improvement of tunable microwave properties is consistent with the reduced compressive strain in the annealed structures fabricated by the three-step method.

## ACKNOWLEDGMENT

This research was funded by a grant from the Office of Naval Research under the direction of Dr. Dan Green.

[1]T. Ji, H. Yoon, J. K. Abraham, and V. K. Varadan, IEEE Trans. Microwave Theory Tech. **54**(3), 1131–1138 (2006).
[2]R. R. Romanofsky, J. T. Bernhard, F. W. Van Keuls, F. A. Miranda, G. Washington, and C. Canedy, IEEE Trans. Microwave Theory Tech. **48**(12), 2504 (2000).
[3]H. Tang, C. Yang, J. Zhang, H. Chen, A. Yu, W. He, and Y. Liao, J. Infrared Millim. THz Waves **31**, 852 (2010).
[4]B. Acikel, Y. Liu, A. Nagra, T. Taylor, P. Hansen, J. Speck, and R. York, IEEE MTT-S Int. Microwave Symp. Dig. **2**, 1191 (2001).
[5]J. H. Leach, H. Liu, V. Avrutin, B. Xiao, Ü. Özgür, H. Morkoç, J. Das, Y. Y. Song, and C. E. Patton, J. Appl. Phys. **107**, 084511 (2010).
[6]P. Suherman, T. Jackson, Y. Tse, I. Jones, R. Chakalova, and M. Lancaster, J. Appl. Phys. **99**, 104101 (2006).
[7]H. Liu, V. Avrutin, C. Zhu, J. Leach, E. Rowe, L. Zhou, D. Smith, Ü. Özgür, and H. Morkoç, Mater. Res. Soc. **1397**, 13 (2012).
[8]B. Xiao, H. Liu, V. Avrutin, J. Leach, E. Rowe, H. Liu, Ü. Özgür, H. Morkoç, W. Chang, L. Alldredge, S. Kirchoefer, and J. Pond, Appl. Phys. Lett. **95**, 212901 (2009).
[9]W. Chang, J. Horwitz, A. Carter, J. Pond, S. Kirchoefer, C. Gilmore, and D. Chrisey, Appl. Phys. Lett. **74**, 1033 (1999).
[10]B. Xiao, V. Avrutin, H. Liu, E. Rowe, J. Leach, X. Gu, Ü. Özgür, H. Morkoç, W. Chang, L. Alldredge, S. Kirchoefer, and J. Pond, Appl. Phys. Lett. **95**, 012907 (2009).
[11]N. A. Pertsev, A. G. Zembilgotov, and A. K. Tagantsev, Phys. Rev. Lett. **80**, 1988 (1998).
[12]W. J. Kim, W. Chang, S. G. Qadri, J. M. Pond, S. W. Kirchoefer, D. B. Chrisey, and J. S. Horwitz, Appl. Phys. Lett. **76**, 1185 (2000).
[13]J. Ha, J. Choi, C. Kang, S. F. Karmanenko, S. Yoon, D. Choi, and H. Kim, Jpn. J. Appl. Phys., Part 2 **44**, L1196 (2005).
[14]L. Yang, G. Wang, X. Dong, and D. Remiens, J. Am. Ceram. Soc. **93**, 2136 (2010).
[15]G. A. Smolenskii and K. I. Rozgachev, Zh. Tekh. Fiz. **24**, 1751 (1954).
[16]N. F. Izyumskaya, V. S. Avrutin, and A. F. Vyatkin, Solid Status Electron. **48**, 1265 (2004).
[17]Y. H. Luo, J. Wan, R. L. Forrest, J. L. Liu, M. S. Goorsky, and K. L. Wang, J. Appl. Phys. **89**, 8279 (2001).
[18]J. H. Leach, H. Liu, V. Avrutin, E. Rowe, Ü. Özgür, H. Morkoç, Y. Y. Song, and M. Wu, J. Appl. Phys. **108**, 064106 (2010).
[19]M. D. Biegalski, D. D. Fong, J. A. Eastman, P. H. Fuoss, S. K. Streiffer, T. Heeg, J. Schubert, W. Tian, C. T. Nelson, X. Q. Pan, M. E. Hawley, M. Bernhagen, P. Reiche, R. Uecker, S. Trolier-McKinstry, and D. G. Schlom, J. Appl. Phys. **104**, 114109 (2008).
[20]W. Chang, C. M. Gilmore, W. J. Kim, J. M. Pond, S. W. Kirchoefer, S. B. Qadri, D. B. Chirsey, and J. S. Horwitz, J. Appl. Phys. **87**, 3044 (2009).
[21]A. Segmuller, J. Vac. Sci. Technol. A **9**, 2477 (1991).
[22]Y. H. Luo, J. Wan, R. L. Forrest, J. L. Liu, G. Jin, M. S. Goorsky, and K. L. Wang, Appl. Phys. Lett. **78**, 454 (2001).
[23]R. N. Simons, *Coplanar Waveguide Circuits, Components, and Systems* (Wiley-Interscience, New York, 2001).
[24]L. Alldredge, W. Chang, S. B. Qadri, S. W. Kirchoefer, and J. M. Pond, Appl. Phys. Lett. **90**, 212901 (2007).
[25]L. Alldredge, W. Chang, S. W. Kirchoefer, and J. M. Pond, Appl. Phys. Lett. **95**, 222902 (2009).
[26]J. Bellotti, W. Chang, S. B. Qadri, S. W. Kirchoefer, and J. M. Pond, Appl. Phys. Lett. **88**, 012902 (2006).